Statistical Characteristics of Turbulent Transport Dominated by Zonal Flow Dynamics

T. MATSUMOTO[1)], Y. KISHIMOTO[2),1)] and J. Q. LI[2)]

1) Japan Atomic Energy Agency, Naka, Ibaraki-ken, 311-0193 Japan
2) Graduate School of Energy Science, Kyoto Univ., Uji, 611-0011, Japan

e-mail: matsumoto.taro@jaea.go.jp

Abstract. Characteristics of ETG-driven turbulent transport dominated by zonal flows and nonlinearly generated large scale structures with low toroidal/poloidal wave numbers are investigated by gyro-fluid simulations in slab geometry. Main results found in this research are as follows. (i) The zonal flows change the characteristics of turbulence from "homogeneous" structure to "inhomogeneous" one, in which micro-scale vortices and nonlinearly generated macro-scale vortices coexist at different radial zones, exhibiting a two-scale nature in turbulence. (ii) The fractal dimension is simultaneously reduced at any radial region with an increase of the ratio of zonal flow energy to that of total fluctuations, accompanied by the disappearance of exponential PDF tail of the heat flux. (iii) The reduction of heat flux in strong zonal flow regime results from two mechanisms in the relation between poloidal electric field and pressure perturbation, *i. e.* the reduction of coherence in the zone of micro-scale vortices and the phase synchronization in that of macro-scale ones. Namely, macro-scale vortices, which is an origin of low fractal dimension and plays a role to saturate zonal flows, is survived in the system without causing large thermal transport by adjusting the phase relation.

1 Introduction

It is important to find key parameters to control the transport dynamics that governs the performance of magnetically confined fusion plasma. In recent years, it has been recognized that transport dynamics is closely related to the structure of turbulence. In particular, large scale structures such as zonal flows (ZF), streamers, generalized Kelvin-Helmholtz (KH) mode, etc, are considered to regulate the turbulent transport in tokamak plasmas [1, 2]. However, the precise roles and underlying physical mechanisms of large scale structures have not been clearly understood.

In order to understand such complex turbulence system, statistical methods have been widely introduced. The fractal dimension was used to characterize the confinement state, such as L and H-modes, attached and detached plasmas, etc [3, 4]. The probability density function (PDF) has been also used both in experiments [5,6] and in theories [7,8] to identify the turbulence. Such a statistical approach may be one of powerful tools in capturing a turbulence state; however the relation between each statistical quantity and corresponding turbulent structure has not yet been fully elucidated.

In this paper, we have investigated the characteristics of electron temperature gradient (ETG)-driven turbulences based on gyro-fluid simulations in slab geometry [2, 9]. Here, we compared the plasmas dominated by ZF with turbulent plasmas, and studied the role of the large scale structure on turbulent transport using statistical methods.

This paper is organized as follows. In Sec.2, we describe our ETG simulation model based on gyrofluid equations and the definition of fractal dimension. In Sec.3, the characteristics of fluctuations and turbulent structure in plasma dominated by ZF are shown. In Sec.4, the dependency of the dimension on magnetic shear, temperature gradient, and the ZF component is discussed. In Sec.5, the PDF of the heat flux is evaluated for various parameters. In particular, the PDF tail components and the similarity of the PDF profile are discussed. In Sec.6, the mechanism of heat flux reduction in plasma dominated by ZF is studied with cross spectrum analysis. Finally, a summary is given in Sec.7.

2 Simulation model and correlation dimension

2.1 Simulation model

In this research, ETG turbulence is modeled based on the following gyro-fluid equation in a sheared slab geometry including Landau damping effect with Hammett-Perkins closure [10] and choosing a proper ion adiabatic response.

$$(1-\hat{\nabla}_\perp^2)\frac{\partial\hat{\phi}}{\partial\hat{t}} = [1+(1+\eta_e)\hat{\nabla}_\perp^2]\frac{\partial\hat{\phi}}{\partial\hat{y}} + [\hat{\phi},\hat{\nabla}_\perp^2\hat{\phi}] + \hat{\nabla}_\parallel\hat{v}_{e\parallel} - \mu_{e\perp}\hat{\nabla}_\perp^4\hat{\phi}, \tag{1}$$

$$\frac{\partial\hat{v}_{e\parallel}}{\partial\hat{t}} = \hat{\nabla}_{e\parallel}\hat{\phi} - \hat{\nabla}_\parallel\hat{p}_e - [\hat{\phi},\hat{v}_{e\parallel}] + \eta_{e\perp}\hat{\nabla}_\perp^2\hat{v}_{e\parallel}, \tag{2}$$

$$\frac{\partial\hat{p}_e}{\partial\hat{t}} = -(1+\eta_e)\frac{\partial\hat{\phi}}{\partial\hat{y}} - [\hat{\phi},\hat{p}_e] - \Gamma\hat{\nabla}_\parallel\hat{v}_{e\parallel} - (\Gamma-1)\sqrt{8/\pi}\mid k_\parallel\mid(\hat{p}_e+\hat{\phi}) + \chi_{e\perp}\hat{\nabla}_\perp^2\hat{p}_e. \tag{3}$$

Here, Γ=5/3, η_e=$d\ln T_e/d\ln n$, and coordinates are normalized to characteristic scales as $\hat{x}$=x/ρ_e, $\hat{y}$=y/ρ_e, $\hat{z}$=z/L_n and $\hat{t}$=$v_{te}t/L_n$. The perturbed quantities, the electrostatic potential, the electron parallel velocity and the electron pressure, are normalized as $\hat{\phi}$=$(L_n/\rho_e)(e\tilde{\phi}/T_e)$, $\hat{v}_{e\parallel}$=$(L_n/\rho_e)(v_{e\parallel}/v_{te})$ and $\hat{p}_e$=$(L_n/\rho_e)(\tilde{p}/p_0)$, with L_n=$(d\ln n/dx)^{-1}$, where ρ_e is the electron Larmor radius, v_{te} is the electron thermal velocity, T_e is the electron temperature, $v_{e\parallel}$ is the electron parallel velocity and n is the electron density. Here, $\hat{p}_e$ includes the zonal component. The magnetic shear parameter $\hat{s}$ is defined as $\hat{s}$=L_n/L_s, where L_s=$B_0/(dB_y/dx)$ and B_0 is the longitudinal magnetic field.

The dynamics of fluid are computed in a three dimensional rectangular box with the Cartesian coordinates (x,y,z). A periodic boundary condition is adopted in y and z directions. The twisting periodicity condition [11] is employed in x direction. The system sizes are mainly set as L_x=$100\rho_e$, L_y=$10\pi\rho_e$, L_z=$2\pi L_n$. For numerically stable and efficient calculation, the viscosity terms is introduced in each equation as a damping effect for the instabilities with wavelength smaller than electron Larmor radius, which does not change the linear growth rate of ETG turbulence. Then, $\mu_{e\perp}$, $\eta_{e\perp}$ and $\chi_{e\perp}$ is assumed to be 0.5. The detail of computation is described in Ref. [12].

2.2 Correlation dimension

To understand the complex dynamics governing intermittent fluctuations in high temperature plasma, the fractal dimension, which is an index of the degree of freedom, have been evaluated. In order to calculate the value of fractal dimension D of the time series data $x(t_i)$ $[i = 1,2,3,\cdots,N]$, it is necessary to reconstruct a trajectory in multi-dimensional space using the embedding theorem. For one-variable time series data, it is appropriate to use time-delay coordinates, *i.e.*,

$$\mathbf{x_i} = \{x(t_i), x(t_i+\tau_{ac}),\cdots,x(t_i+(m-1)\tau_{ac})\}, \tag{4}$$

for noise reduction [13], where m is an embedding dimension and τ_{ac} is the autocorrelation time chosen as an embedding log. In this study, τ_{ac} was defined as the delay, when the autocorrelation function was set at one-half of the value at $\tau = 0$ at the first time point, such that $\langle(x(t)-\langle x\rangle)(x(t+\tau_{ac})-\langle x\rangle)\rangle$= 0.5, where $\langle\cdots\rangle$ denotes the time average.

Although there are several types of fractal dimensions to be defined, it is most appropriate to calculate the correlation dimension D_2 from the point of view of computational feasibility. D_2 can be calculated with Grassberger-Procaccia algorithm [14] by taking the correlation integral of the time series data as follows:

$$C(r) = \lim_{N\to\infty} (1/N^2)\Sigma_{i,j=1}^{N} H(r- \mid \mathbf{x_i} - \mathbf{x_j} \mid), \tag{5}$$

where H is the Heaviside function defined by $H(r) = 1$ for $r \geq 0$ and $H(r) = 0$ for $r < 0$. For each m, $C(r)$ would span a scale such that $C(r) \sim r^{\nu}$. D_2 is obtained as an exponent ν for a necessarily and sufficiently large embedding dimension m.

3 Radial structure of ZF-dominated plasma

In the ETG-driven turbulence, the magnetic shear $\hat{s}$ and temperature gradient η_e are the key parameters to control the large scale structures. Thus, we have performed sheared-slab ETG simulations in various parameter regions, that is, for magnetic shear of $\hat{s} = 0.1\sim0.4$ and electron temperature gradient of $\eta_e = 3\sim6$. For each magnetic shear value, the zonal flow intensity rises as η_e increased. However, the heat flux was not necessarily enhanced with increases in η_e. Thus, it became important to find a means of characterizing turbulent structures that are not necessarily identified by analysis of the ZF intensity.

In the case of quasi-steady state turbulence, a variety of fluctuations are generated through the dynamics of fluctuations with various temporal and spatial scales, and statistical characteristics become uniform in space. However, in the presence of zonal flows, the turbulence is radially restricted by coherent poloidal flows due to the radial electric field, such that the radial transport is reduced. Thus, plasmas dominated by ZF can exhibit different characteristics in the radial direction at the scale length of the Larmor radius.

In the case of turbulent plasma, where the magnetic shear is relatively weak ($\hat{s} = 0.1$) and the electron temperature gradient is small ($\eta_e = 3$), it was found that, after the saturation of linear ETG modes ($t \sim 100L_n/V_{te}$), several modes compete and the ZF component is maintained at levels lower than those competitive modes. On the other hand, in the plasma dominated by ZF, where $\hat{s} = 0.1$ and the electron temperature gradient is large ($\eta_e = 6$), it was found that the ZF component becomes dominant after $t \sim 200$ and gradually increases until $t \sim 700$. From the perspective of energy distribution, it is considered that a quasi-steady state is achieved at approximately $t \sim 1000$ in each case. Thus, the time series data regarding fluctuations from t=1000 to 2000 at the sampling time of 0.01 (L_n/V_{te}) will be used for each statistical analysis hereinafter.

From ETG simulations, in plasma dominated by ZF, which were established in the regime of weak $\hat{s}$ and large η_e, the turbulence displays coherent structure of the electrostatic potential contours, as shown in Fig.1(a). Here, $\hat{s} = 0.1$ and $\eta_e = 6$. However, behind zonal flows, it was found that large vortices moving in the poloidal minus direction are generated by the K-H-like instabilities due to the coupling of background ETG fluctuations and ZF, as shown at the zone (B) in Fig.1(b) (*i.e.* $x = 0$). On the other hand, in the zone (A), in which these the K-H-like instabilities are weak (*i.e.* $x = -12.5$), many small vortices moving in the poloidal plus direction are observed. Therefore, in the presence of ZF, it is expected that the statistical characteristics are dependent on the radial position, due to the formation of the turbulent structure. Namely, small-scale ETG-like vortices (A) and large-scale KH-like vortices (B) are excited at different radial zones and propagate independently in the poloidal direction, since the ZF play a role in disconnecting the radial correlation of the turbulence.

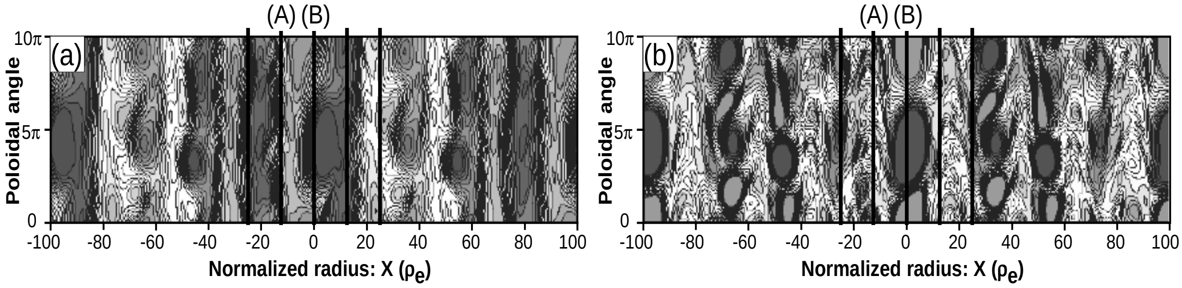

FIG. 1: Contours of the electrostatic potential $\hat{\phi}$ (at t=$1000L_n/V_{te}$) for zonal flow-dominated plasma ($\hat{s}$=0.1, η_e=6) (a) with the zonal flow component and (b) without the zonal flow component. "(A)" and "(B)" denote regions with small and large vortices, respectively.

The radial dependence of the autocorrelation time τ_{ac} of the poloidal electric field $\hat{E}_y$ in the ZF-dominated plasma ($\eta_e = 6$) is shown in Fig.2(a), compared with that in the turbulent plasma ($\eta_e = 3$). It is clear that τ_{ac} is almost uniform in the turbulent state. However, in the plasma dominated by ZF, it is found that τ_{ac} depends considerably on the radial position. In regions with strong K-H-like modes, a relatively long τ_{ac} is obtained, whereas in regions with weak K-H-like modes, τ_{ac} becomes much less long than that in turbulent plasmas. It is therefore evident that the characteristic time scale depends on the radial position in the presence of ZF.

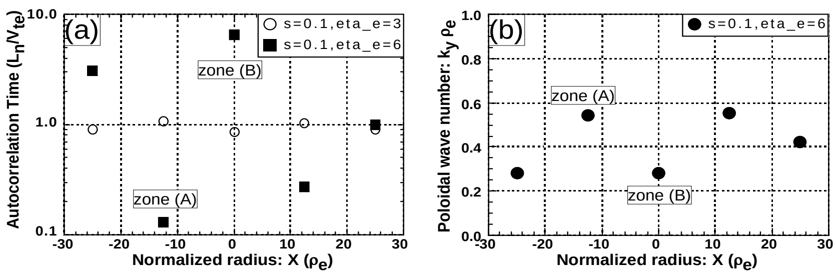

FIG. 2: Radial dependency of the poloidal electric field fluctuations $\hat{E}_y$. (a) Autocorrelation time in the ZF-dominated plasma ($\hat{s}$=0.1, η_e=6) and the turbulent plasma ($\hat{s}$=0.1, η_e=3) are denoted by the closed squares and open circles, respectively. (b) Poloidal wave number in the ZF-dominated plasma is denoted by the closed circles.

Such radial dependency is also observed from the viewpoint of spatial scale. Figure 2(b) shows the radial dependence of the characteristic poloidal wave number $\hat{k_y}$. In the zone (B) with strong K-H-like modes, $\hat{k_y}$ is approximately 0.3. On the other hand, in the zone (A) with weak K-H-like modes, a relatively large $\hat{k_y}$ are obtained.

Thus, ZF change the characteristics of turbulence from homogeneous to inhomogeneous, exhibiting a two-scale nature in turbulence. Hereinafter, we primarily focus on the differences of the statistical characteristics between the zones, (A) and (B), which are typical examples of plasma dominated by ZF.

4 Correlation dimension of fluctuations

To investigate the degrees of freedom inherent in turbulent plasma, the correlation dimension D_2 of fluctuations is evaluated for various parameters. Here, the poloidal electric field fluctuation $\hat{E}_y$ is chosen as the time series data to be analyzed, because $\hat{E}_y$ directly contributes to the radial heat flux via coupling with the pressure perturbation, $\hat{Q} = -\hat{E}_y \hat{p}$.

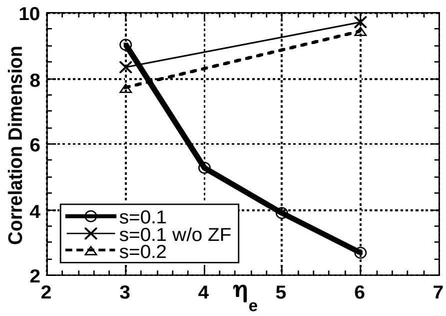

FIG. 3: Correlation dimension of the poloidal electric field $\hat{E}_y$ for different electron temperature gradient η_e. The open circles, triangles and crosses denote the cases with $\hat{s} = 0.1$, 0.2, and 0.1 without the ZF component, respectively.

To understand the parameter dependency of D_2, for the magnetic shear of $\hat{s} = 0.1, 0.2$, and 0.1 without ZF component, D_2 is plotted as a function of η_e in Fig. 3. For the weak magnetic shear cases ($\hat{s} = 0.1$), in the case of a small temperature gradient ($\eta_e = 3$) where the ZF intensity is small, it was found that D_2 becomes relatively high ($D_2 = 8 \sim 9$). Thus, the turbulent plasma with large intermittency has a corresponding large degree of complexity. As η_e increases, it was also observed that D_2 decreases significantly. In particular, D_2 becomes approximately 3 to 4 in plasma dominated by zonal flows with a large temperature gradient ($\eta_e = 6$), where the time series data exhibit dominant periodic oscillation with small intermittency, as the ZF excited by ETG turbulence drive K-H-like instabilities. The reduction of the dimensionality was observed at each radial point, nevertheless the plasma is inhomogeneous and the spatiotemporal scale of fluctuations significantly varied in radial direction, as mentioned in Sec.3.

By comparing D_2 at $\eta_e = 3$ and 6 in the $\hat{s} = 0.1$ plasmas without the ZF component, it was found that the pure temperature gradient effect is small ($\Delta D_2 \sim 1$). The increase in η_e without the ZF component does not contribute much to the statistical behavior of turbulent fluctuations, although the average amplitude of $\hat{E}_y$ fluctuations is enhanced several-fold. Thus, the degree of complexity does not changed substantially, although the electron heat conductivity is significantly enhanced. Next, by comparing D_2 with and without the ZF component, but at the same parameters of $\hat{s} = 0.1$ and $\eta_e = 6$, it becomes clear that D_2 is significantly reduced, and $\Delta D_2 = 6{\sim}7$. Then, the pure effect of ZF dominancy is found to induce a large reduction in the degree of freedom inherent in turbulent plasma. For relatively large magnetic shear ($\hat{s} = 0.2$), D_2 is gradually enhanced by increasing η_e, as well as D_2 for $\hat{s} = 0.1$ without ZF component. This is because the fluctuations at $\hat{s} = 0.2$ still exhibit large intermittency even for $\eta_e = 6$.

The above results demonstrated that D_2 sufficiently reflects the variation in turbulent characteristics such as ZF dominancy. Therefore, it is possible to identify some aspects of turbulent structures by evaluating the dimensionality of the fluctuations.

5 Probability density function of fluctuations

In recent years, the PDF analysis of fluctuation amplitude has the focus of attention in attempts to evaluate characteristics of turbulent plasmas. The deviation of the PDF values from the Gaussian profile shows the behavior of the fluctuation amplitude to a much greater degree than does the skewness or the flatness of fluctuations, and the inclination of the PDF tail has been found to characterize the degree of intermittency.

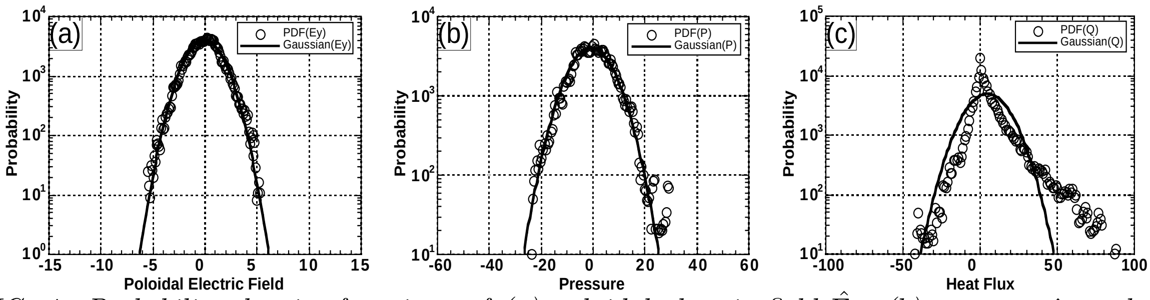

FIG. 4: Probability density functions of (a) poloidal electric field $\hat{E}_y$, (b) pressure $\hat{p}$, and (c) heat flux $\hat{Q}$ in the turbulent plasma with $\hat{s} = 0.1$ and $\eta_e = 3$.

At first, the PDF of $\hat{E}_y$, $\hat{p}$, and $\hat{Q}$ are investigated in the turbulent plasma ($\hat{s} = 0.1$, $\eta_e = 3$), as shown in Fig.4. It is observed that the PDF of $\hat{E}_y$ is in good agreement with a Gaussian profile with the same standard deviation and average value as those of the $\hat{E}_y$ time series data. The PDF of $\hat{p}$ is also found to be similar to the Gaussian profile, although there is some deviation in the positive large amplitude region. However, it was clarified here that the PDF of $\hat{Q}$ exhibits a strong deviation from the Gaussian profile. The large tail component in the positive region, generated by the phase coupling between $\hat{E}_y$ and $\hat{p}$, indicates the existence of intermittent heat pulses that are larger those that predicted from the Gaussian probability, which can be observed as the large spiky bursts in the time series data. Thus, the magnitude of $\hat{Q}$ tail component closely contributes to the net heat transport.

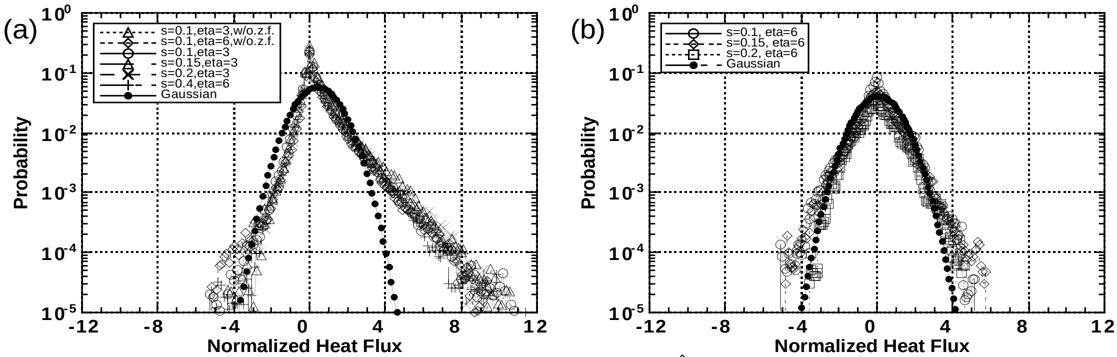

FIG. 5: Probability density functions of the heat flux $\hat{Q}$ for (a) turbulent plasmas, and (b) ZF-dominated plasmas.

Next, Fig.5 shows the PDF of $\hat{Q}$ in various parameter regions with $\hat{s} = 0.1{\sim}0.4$ and $\eta_e = 3{\sim}6$, including the cases without the ZF component. In each case, the horizontal axis indicates a heat pulse normalized with the standard deviation obtained from the population of each time series data set, and the vertical axis shows a normalized probability, such that the integral of PDF over the heat flux arrives at 1. Here, a Gaussian profile is plotted as a reference. It was obvious that the behavior of the PDF of $\hat{Q}$ can be classified into one of two different categories.

In turbulent plasmas, in which several modes compete and a turbulent structure is maintained, the PDF is found to have a typical shape with a clear exponential tail which manifests intermittent transport, as shown in Fig.5(a). The tail component has $\exp(-Q^1){\sim}\exp(-Q^{3/2})$ dependency, which is consistent with a theoretical prediction [7]. In particular, a prominent similarity to each other in the normalized PDF profile, which is insensitive to plasma parameters such as $\hat{s}$ and η_e. Thus, such a similarity of heat flux PDF in turbulent plasmas may be a unique nature of intermittent fluctuations.

On the other hand, the exponential PDF tail is reduced in plasmas dominated by ZF, as shown in Fig.5(b). It was also confirmed here that the symmetry with respect to the sign of amplitude is recovered, such that the net turbulent transport is decreased. In this case, the PDF does not become an inherent Gaussian.

From the above results, the variation in turbulent characteristics such as intermittency appears to be well reflected in the PDF of $\hat{Q}$, and in particular, at the tail component. It is thus considered useful to evaluate the PDF of fluctuations in order to identify certain aspects of turbulent structures, such as experimental identification of large scale structures.

6 Causality of reduction of heat flux

From the cross spectrum analysis between $\hat{E}_y$ and $\hat{p}$ in turbulent plasma and in plasmas dominated by ZF, we have clarified their correlation relation generating the net heat flux. Figure 6 (a) shows that a relatively high coherency in broad frequency regime, which manifests the production of net heat flux, is observed in the turbulent plasma, in which such high coherency may be homogeneously observed.

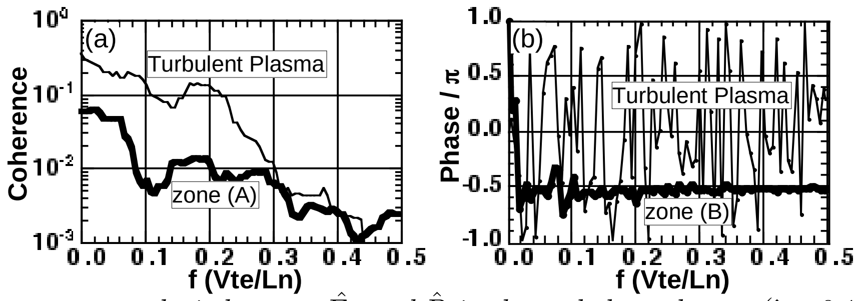

FIG. 6: Cross spectrum analysis between $\hat{E}_y$ and $\hat{P}$ in the turbulent plasma ($\hat{s} = 0.1$ and $\eta_e = 3$) and in the ZF-dominated plasma ($\hat{s} = 0.1$ and $\eta_e = 6$). (a) Reduction of coherence from turbulent plasma (thin line) to (A) small vortices zone (thick line). (b) Synchronization of phase difference from turbulent plasma (thin line) to (B) large vortices zone (thick line).

On the other hand, in the plasma dominated by ZF, the cross spectrum analysis shows radially dependent results proceeding from different spatiotemporal characteristic scales. At the zone (A), in which background ETG-like modes induce small vortices (Figs.1 and 2), it was found that the coherence is significantly reduced in wide spectrum range, compared with that in the turbulent plasma, as shown in Fig.6(a). Such reduction of coherence is considered to correspond to the reduction of net heat flux.

At the zone (B), in which K-H-Like modes induce large vortices, the coherence is not reduced. Alternatively, the phase difference between $\hat{E}_y$ and $\hat{p}$ is found to be considerably regulated by ZF, as shown in Fig.6(b). As a result, the phase difference becomes approximately $-\pi/2$, which means that net heat transport is significantly reduced.

Thus, it is concluded that, in ETG turbulent plasma dominated by ZF, the reduction of heat flux is conducted by two exclusive mechanisms, i.e., the reduction of coherence and the phase synchronization between $\hat{E}_y$ and $\hat{p}$.

7 Summary and Conclusions

In order to gain a better understanding of the turbulent dynamics in tokamak plasmas dominated by ZF and K-H like modes, the ETG turbulence was simulated with a gyrofluid model in a sheared-slab configuration. In ZF-dominated plasmas, it was found that the spatiotemporal characteristic scales with respect to local turbulent fluctuations are regulated by the alternative existence of two kinds of zones with large vortices induced by K-H-like modes and small vortices induced by background ETG-like modes, respectively.

The correlation dimension of fluctuations, which is relatively high (9∼10) in turbulent plasmas, is significantly reduced to 3∼4 by the increase of ZF dominancy. The reduction of the dimensionality was observed at each radial point over two different spatiotemporal scales. This result shows that the fluctuations in the plasma dominated by ZF are not sustained by random processes [15].

In turbulent plasmas, the prominent exponential tails of heat flux PDF were observed, which manifests an intermittent transport dynamics with a large heat flux. The PDF tail were found to exhibit strong similarity, which is insensitive to plasma parameters such as $\hat{s}$ and η_e unless ZF is strongly excited. It was also found that, as the ZF intensity increases, the exponential tail disappears and the PDF becomes almost symmetric, such that the net turbulent heat transport is decreased.

In plasmas dominated by ZF, the cross spectrum analysis between $\hat{E}_y$ and $\hat{p}$ shows radially different results. It is found that, in turbulent plasmas dominated by ZF, the restriction of heat flux is conducted by two mechanisms, *i.e.*, the reduction of coherence in wide spectrum range and the phase synchronization between $\hat{E}_y$ and $\hat{p}$.

Acknowledgements

The authors would like to express their gratitude to Drs. M. Kikuchi, Y. Miura and M. Azumi (JAEA) for their useful suggestions. This study was partly supported by Grant-in-Aid from the Japan Society for the Promotion of Science (No. 16760683).

References

[1] P.H.Diamond, S.-I.Itoh, et al., Plasma Phys. Cont. Fusion, 47 (2005) R35.

[2] J.Li and Y.Kishimoto, Phys. Plasmas, 9, 1493 (2004).

[3] A. Komori, et al., Phys. Rev. Lett., **73**, 660 (1994).

[4] V. Budaev, et al., Plasma Phys. Cont. Fusion, **35**, 429 (1993).

[5] G. Y. Antar, et al, Phys. Rev. Lett., **87**, 065001 (2001).

[6] O. E. Garcia, et al., Plasma Phys. Cont. Fusion, **45**, 919 (2003).

[7] E. Kim, P. H. Diamond, M. Malkov, et al., Nuclear Fusion, **43**, 961 (2003).

[8] S-I. Itoh, et al., J. Phys. Soc. Jpn., **68**, 1891, 2611 (1999); **69**, 408, 3253 (2000).

[9] T.Matsumoto, Y.Kishimoto, J.Li, Proc. 19th ICNSP and 7th APPTC, (2005) 258.

[10] Hammett G. W. and Perkins F. W. 1990 *Phys. Rev. Lett.* **64**, 3019.

[11] Beer M.A., Cowley S.C. and Hammett G.W. 1995 *Phys. Plasmas* **2**, 2687.

[12] Li J. and Kishimoto Y. 2002 *Phys. Plasmas* **9**, 1241.

[13] N. H. Packard, et al., Phys. Rev. Lett., **45**, 712 (1980).

[14] P. Grassberger and I. Procaccia, Phys. Rev. Lett., **50**, 346 (1983).

[15] Z.Lin, S.Ethier, T.S.hahm, et al., Phys. Rev. Lett., 88 (2002) 195004.